PHYSICAL REVIEW VOLUME 136, NUMBER 1A 5 OCTOBER 1964

Interaction of Transverse Acoustic Waves [$\hbar\omega \ll \varepsilon_0(0)$] with Real Fermi Surfaces in Superconductors

J. R. LEIBOWITZ†
Westinghouse Research Laboratories, Pittsburgh, Pennsylvania
(Received 23 March 1964)

A model is proposed which attempts to treat seemingly conflicting results obtained recently in experiments involving attenuation of transverse acoustic waves by electrons in a number of superconductors. The electron-transverse wave interaction is described in the superconducting state immediately below T_c by turning off the electromagnetic interaction within the Pippard formalism, which treats the normal state. There is obtained in this way a model for the residual superconducting attenuation by electrons which contains explicitly both the collision-drag and shear-deformation contribution. It is shown that the interaction with shear waves in the superconducting state is reduced to a simple form when $ql \gg 1$, so that it is possible to study the shear-deformation tensor in a rather direct way; the superconducting shear-wave electronic attenuation for $ql \gg 1$ is found to reduce to the same form as the corresponding normal-state compressional-wave attenuation. The model is applied in an examination of general features of experimental data on tin, aluminum, gallium, and some transition metals. In application of the model to aluminum, for the case of a given propagation orientation, Fermi surface deformation is found to account for roughly 10% of the total electronic interaction at low temperatures. Finally, the form obtained for the shear-deformation contribution to the residual attenuation is shown to suggest the applicability of the Bardeen, Cooper, Schrieffer (BCS) relation to the case of superconducting transverse-wave residual attenuation when $ql \gg 1$.

I. INTRODUCTION

A MODEL is proposed which attempts to treat seemingly conflicting results obtained recently in experiments involving attenuation of transverse ultrasonic waves by the "normal" electrons, viz., the excited quasiparticles, in a number of superconductors. The analysis was motivated by some experimental results which we have obtained in superconducting tin,[1] and the aluminum data of David, van der Laan, and Poulis.[2] In particular, David and co-workers found deviations of their results from free-electron theoretical predictions (see later). We felt that these discrepancies were attributable to shear-deformation interactions. But in order to make a quantitative application of these ideas, it became necessary to carry out an analysis which takes explicit account of the shear-deformation effect. The electron-shear wave interaction is described immediately below T_c, the superconducting transition temperature, by turning off the electromagnetic interaction within the Pippard[3] formalism, which treats the normal state. There is obtained a model for the residual superconducting attenuation by electrons which contains explicitly both the collision-drag and the shear-deformation contribution.

Before proceeding, it will prove helpful to introduce briefly the relevant phenomena associated with electron interaction of transverse acoustic waves in a superconductor. When the wave number q of the ultrasonic wave and the electron mean free path l are sufficiently large, viz., when $ql \sim 1$, interaction with electrons can be the dominant source of ultrasonic attenuation in a metal at low temperatures. This condition is generally attainable at megacycle frequencies, in very pure metals, in the liquid-helium temperature range. When $ql \gg 1$, the problem, when involving compressional waves, reduces to the standard quantum mechanical problem of inelastic scattering of electrons and phonons under the influence of a simple interaction potential.[4] A number of workers have treated aspects of the more general problem,[5] involving arbitrary ql and Fermi surface, for the case of the normal-state interaction.

Longitudinal-wave ultrasonic attenuation dominated by electron interaction at helium temperatures was first observed in 1954.[6,7] While it was recognized that the rapid attenuation decrease in the superconducting state reflected the decreasing normal electron population, it was not until the development of the Bardeen, Cooper, Schrieffer theory (hereafter, BCS),[8] in 1957, that it became possible to account for the form of the temperature dependence of the superconducting-state attenuation. Thus it was determined from measurement of the superconducting attenuation of longitudinal waves in tin, by Morse *et al.*[9] in 1957, that the BCS relation

$$\frac{\alpha_{sl}}{\alpha_{nl}} = 2F(\Delta) = \frac{2}{e^{\Delta/kT}+1} \tag{1}$$

is rather well satisfied experimentally; α_{sl} and α_{nl} are

† Present address: Department of Physics and Astronomy, University of Maryland, College Park, Maryland.
[1] J. R. Leibowitz, Phys. Rev. **133**, A84 (1964).
[2] R. David, H. R. van der Laan, and N. J. Poulis, Physica **29**, 357 (1963).
[3] A. B. Pippard, Proc. Roy. Soc. (London) **A257**, 165 (1960).
[4] See the review article by R. W. Morse, *Progress in Cryogenics* (Heywood and Company, Ltd., London, 1959), Vol. I.
[5] A. B. Pippard, Phil. Mag. **46**, 1104 (1955); also see, for example, Ref. 3, and R. G. Chambers, in *Proceedings of the Seventh International Conference on Low Temperature Physics*, edited by G. M. Graham and A. C. H. Hallett (The University of Toronto Press, Toronto, 1961).
[6] H. E. Bömmel, Phys. Rev. **96**, 220 (1954).
[7] L. MacKinnon, Phys. Rev. **98**, 1181, 1210 (1955).
[8] J. Bardeen, L. N. Cooper, and J. R. Schieffer, Phys. Rev. **108**, 1175 (1957).
[9] R. W. Morse and H. V. Bohm, Phys. Rev. **108**, 1094 (1957).

the longitudinal-wave attenuation coefficients in the superconducting and normal states, respectively, and F is the Fermi function of the temperature-dependent superconducting energy gap Δ. Equation (1) applies when the phonon energy $\hbar\omega$ is very small compared with the $0°K$ energy gap $\Delta(0)$, and is restricted in the original BCS treatment to the case of longitudinal waves satisfying the condition $ql > 1$. A subsequent generalization by Tsuneto[10] demonstrated that a relation of the same form as Eq. (1) should apply for all ql in the case of longitudinal-wave attenuation.

It was soon found[11] that the attenuation of transverse waves exhibited quite different behavior in the region immediately below T_c. As temperature was reduced below T_c in polycrystalline indium and tin there was observed an initial very sharp drop in the transverse-wave superconducting attenuation α_{St} followed by a much more gradual decrease with temperature (see Fig. 1). Since the temperature range ΔT corresponding to the "rapid-fall" region was very small, i.e., $\Delta T/T \ll 1$, α_{St} appeared to decrease almost discontinuously initially; a 55% drop was observed with a temperature decrease of 0.01°K below T_c, while it decreased only by 4% on further cooling through the next 0.02°K. It was also observed that the "discontinuity" became somewhat smaller with reduction of ql. The residual attenuation $\alpha_r(T)$, the attenuation remaining below the rapid-fall region, was found to satisfy the BCS relation, Eq. (1), about as well as did the longitudinal attenuation. These observations on transverse waves in tin have been confirmed by several observers.[1,12]

In an effort to improve understanding of the rapid-fall region Claiborne[13] made detailed observations on the ultrasonic attenuation of transverse waves near T_c in superconducting aluminum. It was determined that the decrease in α_{St} just below T_c, although very rapid, was not discontinuous, but that the temperature range of the rapid-fall region extended to $\sim 0.001t$ below T_c; t is the reduced temperature T/T_c. It was also shown, using a formalism similar to that of Holstein[14] that the "collision-drag" effect could account for the presence of a residual attenuation. "Collision drag"[14,15] refers to the tendency of the electron distribution, perturbed by the injected lattice wave, to relax to a distribution centered not on the zero of velocity but rather on the local particle velocity $\mathbf{u}$ associated with the lattice wave. When the dissipative interaction associated with collision drag was introduced in an ideal free-electron theory, a

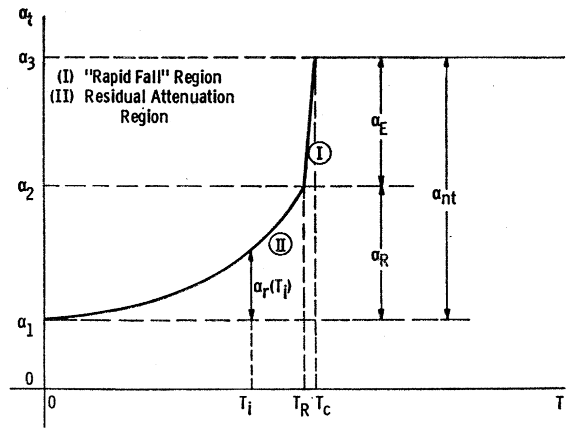

FIG. 1. Schematic representation of shear-wave electronic attenuation α_t versus temperature T.

frequency-dependent residual attenuation was found. Thus, defining α_R as the total residual attenuation (see Fig. 1), Claiborne and Morse concluded that

$$\alpha_R = g\alpha_{nt}, \tag{2}$$

where

$$g = \frac{3}{2(ql)^2}\left\{\frac{(ql)^2+1}{ql}\arctan(ql) - 1\right\}; \tag{3}$$

g is identical with the parameter which appears in Pippard's[5] free-electron treatment of the transverse-wave normal-state attenuation α_{nt} in which theory

$$\alpha_{nt} = K[(1-g)/g], \tag{4}$$

where K is a constant for a given metal. Further, on the assumption that the BCS temperature dependence for the compressional-wave absorption coefficient [see Eq. (1)] could be applied here, it was predicted that

$$\alpha_r(T_i)/\alpha_{nt} = g \times 2F[\Delta(T_i)], \tag{2'}$$

for temperatures lying within the residual attenuation region; $\alpha_r(T_i)$ refers to the residual attenuation remaining at temperature T_i.

II. RECENT EXPERIMENTS: APPARENT ANOMALIES

Until fairly recently there had been observed no qualitative exception to the original observations on electron interaction with transverse ultrasonic waves in superconductors, viz., the appearance of the two rather distinct regions described earlier, in the temperature dependence of the attenuation below T_c. In some recent experiments, however, there have been recorded a number of instances for which no clear separation into "rapid-fall" and "residual" attenuation regions could be made; and in others, though such a separation was possible, apparent behavioral discrepancies among the several experimental cases examined pointed up the need for a better understanding of the physical mecha-

[10] T. Tsuneto, Phys. Rev. **121**, 402 (1961).
[11] See Ref. 4.
[12] A. R. Mackintosh, in *Proceedings of the Seventh International Conference on Low Temperature Physics*, edited by G. M. Graham and A. C. H. Hallett (The University of Toronto Press, Toronto, 1961).
[13] L. T. Claiborne, Ph.D. thesis, Brown University, 1961 (unpublished); R. W. Morse, IBM J. Res. Develop. **6**, 58 (1962).
[14] T. Holstein, Research Memo 60-94698-3-M17, Westinghouse Research Laboratories, Pittsburgh, Pennsylvania, 1956 (unpublished).
[15] T. Holstein, Phys. Rev. **113**, 479 (1959).

nisms governing the separation into the two regions observed in the superconducting state.

Among these results are the recent data on shear-wave electronic attenuation in some of the superconducting transition elements. Levy, Kagiwada, and Rudnick[16] failed to see a sharp fall-off region near T_c in vanadium and niobium single crystals. Measurements were made in the frequency range 75 to 225 Mc/sec on samples estimated to have resistance ratios, $\rho 300°\mathrm{K}/\rho 4.2°\mathrm{K}$, of approximately 8 and 150 for Nb and V, respectively; it was determined that $ql \ll 1$ in those measurements. Similarly, in shear-wave measurements on niobium by Dobbs (private communication) no sharp fall-off region was found. Although the resistivity ratio of the niobium (approximately 500) in the measurements of Dobbs was considerably higher than in the above mentioned case, it was estimated that the condition $ql<1$ was still applicable in these experiments.

At the same time it is necessary to recall the results of Hart and Roberts,[17] on high-purity gallium single crystals. In contrast to the data cited above for vanadium and niobium, $ql \gg 1$ in the measurements on gallium, Hart and Roberts estimated $ql>100$ for all frequencies used in the measurements. For most orientations of the lattice wave relative to the gallium crystal axes there were observed distinct regions of rapid fall and residual attenuation, of comparable magnitude. Yet Eqs. (2) and (3) predict that $\alpha_R/\alpha_{nt}\approx 0$ for such large values of ql.

In addition to the experimental evidence related to the presence or absence of a rapid-fall region in the shear-wave electronic attenuation in superconductors, it is necessary also to cite, for those cases in which both regions do occur, recent observations on the relative magnitude of the residual-attenuation and rapid-fall region, and the parameters which have been observed to affect them. It was noted in Sec. I that the earliest observations on the temperature dependence of transverse-wave attenuation, in polycrystalline indium and tin, indicated that the relative magnitude of the residual-attenuation and rapid-fall regions was dependent on frequency. It was also pointed out that, in examining this frequency effect in aluminum, Claiborne and Morse determined that the presence of a residual attenuation $\alpha_r(T)$ and the frequency dependence of α_r/α_{nt} were assignable to the collision-drag interaction between the electron and lattice-wave systems. The later measurements by Hart and Roberts in gallium, cited above, indicated that there was no frequency dependence of the relative magnitudes of attenuation in the two regions; the ratio $\alpha_r(T)/\alpha_{nt}$ showed no dependence on frequency, even though frequency ranged from roughly 10 to 300 Mc/sec.

[16] M. Levy, R. Kagiwada, and I. Rudnick, in *Proceedings of the Eighth International Conference on Low Temperature Physics*, edited by R. O. Davies (Butterworths Scientific Publications, Inc., Washington, D. C., 1963).

[17] H. R. Hart, Jr., and B. W. Roberts, Bull. Am. Phys. Soc. 7, 175 (1962).

Further, in a recent experimental study of aluminum by David *et al.*,[2] the results were found to be in conflict with the description embodied in Eq. (2): Although the residual attenuation did depend on frequency, the dependence appeared to deviate significantly from the predictions of Eq. (2). And in an experimental study of the transverse wave electronic attenuation in superconducting tin,[1] we found evidence to suggest that a frequency-independent term, large in the case of tin, must be included (in addition to that identified with collision drag) in order to adequately describe $\alpha_r(T)/\alpha_{nt}$. Further discussion of this matter is deferred to a later section.

In summary, then, the experimental evidence has provided the following picture for the absorption of transverse acoustic waves by the excited quasiparticles in a number of superconductors. Although a rapid-fall region immediately below T_c is characteristic of the transverse-wave attenuation, it may not occur in particular instances. In the transition metal results, for which $ql<1$ thus far, α_{St}/α_{nt} is not separable into distinct rapid-fall and residual-attenuation regions. This result may be understood on the reasoning represented by Eqs. (2) and (3). However, although it would appear from Eq. (2) to be required that the relative electronic attenuation associated with the residual region be frequency-dependent, a large but frequency independent α_R/α_{nt} was observed by Hart and Roberts in gallium. And finally, David *et al.* suggest that Eq. (2) gives an incorrect account of the observed ql dependence of $\alpha_r(T)/\alpha_{nt}$ in aluminum.

It has been recognized that the "rapid-fall" behavior in the shear-wave attenuation immediately below T_c is attributable to Meissner effect,[18] and that collision-drag and shear-deformation effects can make contributions to the total observed electronic attenuation. However, the predictions embodied in Eq. (2) are based on an ideal free-electron treatment, and therefore necessarily omit the effects associated with shear deformation of the Fermi surface. In order to treat the experimental results summarized above it is necessary to describe both collision-drag and shear-deformation effect simultaneously in a consistent manner; the relative importance of these effects depends on properties associated with a given Fermi surface (see later), and, in a given metal, on the observed ql range. That the shear-deformation interaction can be most significant was seen in a study of superconducting shear-wave attenuation in tin.[1]

III. THE SHEAR-WAVE INTERACTION

A. The Pippard Theory for the Normal State

In order to examine the phenomena noted in the foregoing discussion it is necessary to treat the problem of

[18] See, for example, the review by J. Bardeen and J. R. Schrieffer, in *Progress in Low Temperature Physics*, edited by C. J. Gorter (North-Holland Publishing Company, Amsterdam, 1961), Vol. III, p. 170.

the interaction of an arbitrary Fermi surface with transverse acoustic waves. The temperature region of interest is in the immediate vicinity of T_c, the superconducting transition temperature. It is of interest, for this case, to consider the Pippard theory[19] for normal-state attenuation of acoustic waves by an arbitrary Fermi surface. A model for the transverse-wave interaction with an arbitrary Fermi surface in the superconducting state at T_c is obtained by turning off the electromagnetic interaction within the Pippard formalism.

The interactions between the lattice and the electrons associated with passage of a lattice wave are considered in the Pippard theory[20] for the normal-state attenuation, from the point of view of a reference frame fixed in the lattice. Transformation to this noninertial frame involves the appearance of fictitious forces arising from two separable mechanisms. The first, the so-called "relative-velocity effect," is associated with the apparent change in **k** of a given electron as measured by observers at rest in the lattice but located at different points along the trajectory of an electron, and hence making their observations at different times. The shifting lattice is responsible for an apparent change of propagation vector **k** of an electron, and thus causes it to be subjected to a fictitious force $\pi_i^{(1)}$. The component along the path of the electron, $\pi^{(1)}=\pi_i^{(1)}n_i$ where n_i is the component of unit vector **n** along the path, would, for the case of uniform strain, represent the force causing the electron to leave the Fermi surface.

An additional fictitious force π^2 arises when the strain is nonuniform and time varying. When gradients of strain are present, the Fermi surface itself changes in shape. Under equilibrium conditions, viz., static strain, an electron can of course remain on the Fermi surface. But when the lattice strain is time varying, an additional fictitious force appears which acts to make an electron leave the Fermi surface, since the shape of the Fermi surface is changing as the electron moves from point to point in k space. The change in shape of the Fermi surface under lattice strain may be described by a deformation parameter K_{ij}, defined by the relation

$$\Delta k_n = K_{ij}\bar{\omega}_{ij}; \tag{5}$$

$\bar{\omega}_{ij}=\partial\xi_j/\partial x_i$ denotes the state of strain, ξ_j being the particle displacement and x_i, translation along the propagation direction. Δk_n is the normal displacement of the Fermi surface associated with the deformation, determined at each point of the Fermi surface by the deformation parameter K_{ij}. Deformations are small and related linearly to changes in the Fermi surface. The two fictitious forces, acting normal to the Fermi surface, viz., parallel to the motion of the electron, are found to be given by

$$\pi^{(1)}=i\hbar n_i q_i u_j k_j, \tag{6}$$

and

$$\pi^{(2)}=i\hbar q_i K_{ij} u_j; \tag{7}$$

$u_j=\dot{\xi}_j$, the particle velocity; q_i is the propagation vector of the lattice wave.
The resultant force π' is then

$$\pi'=\pi^{(1)}+\pi^{(2)}=i\hbar q_i u_j D_{ij}, \tag{8}$$

where

$$D_{ij}=n_i k_j + K_{ij}.$$

The force π' tends to cause electrons to leave the Fermi surface and hence set up a net current, which, from the point of view of an observer fixed in the lattice, is purely electronic.

However, for the frequencies of interest in the present considerations, viz., below frequencies of the order of 1000 Mc/sec, no net current can flow: No space charge can be established at frequencies below the plasma frequency range; and, as for transverse currents, although the condition is less stringent, the assumption of zero current is a good one in ordinary metals (Fermi velocities $\sim 10^8$ cm/sec) below acoustic frequencies of the order of 1000 Mc/sec. Hence it is necessary that an electric field **E** be set up such that there is no net electronic current relative to the lattice; under the combined influence of π' and **E** a current quasibalance condition is established. Pippard assumes a relaxation time to exist at all points, and, from calculation of the rate of dissipation of excess energy of the displaced electron assembly, obtains for the normal-state attenuation of the acoustic wave by the electron system

$$\alpha=\frac{\hbar q}{4\pi^3 M v_s}\left\{\int\frac{\mathfrak{D}^2 a\,dS}{1+(a)^2\cos^2\varphi}+\frac{e^2}{4\pi^3\hbar q}\rho_{ij}{}^q I_i I_j\right\};$$
$$I_i=\int q l_i\left(\frac{\mathfrak{D}a\cos\varphi}{1+(a)^2\cos^2\varphi}\right)dS. \tag{9}$$

M is the density of the metal, and v_s is the sound velocity; φ is the angle between **v** and **q**, **v** being the Fermi velocity; l_1 is the vector mean free path; and $\mathfrak{D}=\mathbf{D}\cdot(\mathbf{u}/u)$, the component of **D** in the particle-velocity direction of the acoustic wave. Finally, the parameter $\rho_{ij}{}^q$ is the resistivity tensor of the periodic electric field associated with the acoustic wave, characterized by wave number q. In Eq. (9) the product ql has been represented by the symbol a.

B. A Model for the Superconducting Shear-Wave Interaction

In Fig. 1 are represented some of the parameters which will prove useful. The regions of interest and the relevant parameters may be distinguished to a sufficient degree of precision as follows. The attenuation coefficient α_1 represents the nonelectronic attenuation, which is

[19] A. B. Pippard, in *The Fermi Surface,* edited by W. A. Harrison and M. B. Webb (John Wiley & Sons, Inc., New York, 1960); Proc. Roy. Soc. (London) **A257**, 165 (1960); also see Ref. 3.
[20] In interest of clarity, relevant arguments from Refs. 3, 19 are presented in very brief outline. The notation is preserved.

temperature independent in the liquid-helium region.[21] The difference $\alpha_3-\alpha_1$, the total (or normal-state) electronic attenuation at temperature T_c, the superconducting critical temperature, is represented by $\alpha_n(T_c)$. The region of interesction of the rapid-fall and residual-attenuation zones, labeled (I) and (II), respectively, is indicated by attenuation coefficient α_2 and temperature T_R. The attenuation change represented by $\alpha_2-\alpha_1$ is the total residual attenuation α_R, the maximum electronic attenuation occurring in region (II); and $\alpha_r(T_i)$ represents the residual electronic attenuation remaining at temperature T_i. Thus, $\alpha_R=\alpha_r(T_R)$. Finally, α_E is that portion of the electronic attenuation associated with region (I). For convenience in displaying the two regions, the separation T_C-T_R, i.e., the "width" of region (I), has been greatly exaggerated in the figure. From experiment and theory[4,10,12,13] the separation is found to be given by $(T_C-T_R)/T_C\sim 0.001$. For the purposes of the following discussion, allowing T_R and T_C to coincide and letting the attenuation in region (I) fall discontinuously from α_3 to α_2, will prove to be a useful simplification which has no effect on the results.[22] Thus, the superconducting-to-normal attenuation ratio is given as follows:

$$\frac{\alpha_{st}}{\alpha_{nt}}(T_i)\approx\frac{\alpha_r}{\alpha_{nt}}(T_i),\quad 0\leq T_i<T_c, \tag{10}$$

and

$$\frac{\alpha_s}{\alpha_{nt}}(T_c)=\frac{\alpha_E}{\alpha_{nt}}+\frac{\alpha_R}{\alpha_{nt}}=1. \tag{11}$$

It will be shown for the general case of real Fermi surfaces that α_R/α_{nt} and α_E/α_{nt} have the following properties:

(1) α_R/α_{nt} goes to 1 when a becomes much smaller than 1. Thus, by definition α_E/α_{nt} goes to zero. (Recall that $a\equiv ql$.)

(2) As a increases α_R/α_{nt} becomes reduced in magnitude, until for $a\gg 1$, α_R/α_{nt} approaches a constant value, α_D/α_{nt}.

(3) α_D is related in a rather simple way to the shear deformation parameter K_{xy}. Thus,

$$\alpha_D\approx\frac{\hbar q}{4\pi^2 M v_s}\oint RK_{xy}{}^2 d\psi,$$

where R is the product of the principal radii of curvature and the integral is taken about the so-called "effective zones," which will be described presently.

(4) If the free-electron limit is taken, it is found that α_R/α_{nt} reduces to g, in agreement with the free-electron model of Morse and Claiborne.

[21] See, for example, Ref. 4.

[22] Even on the assumption of a BCS temperature dependence, which is very sharp near T_c, the approximation results in an error $\sim 1\%$ in determination of α_R/α_n since $(T_c-T_R)/T_c\sim 0.001$.

The electromagnetic interaction. At the time of the first observations by Morse *et al.*[4] of a rapid-fall region in the superconducting shear-wave electronic attenuation it was suggested that the rapid attenuation change near T_c must be associated with a "shorting out" of the local electric fields by the superconducting electrons. It is of interest for present purposes to consider here the peculiar sensitivity of the transverse wave interaction, relative to the longitudinal wave one, to the onset of the superconducting state. The passage of the injected lattice wave through the specimen is associated with a spatial and temporal modulation of lattice points. Assuming a sinusoidal modulation, the particle velocity $\mathbf{u}$ will have a wave-like dependence of the form $\exp[i(qx-\omega t)]$. We assume either pure longitudinal or pure transverse waves. The associated local electric fields, arising as a consequence of the separation of ionic cores from their electronic environment, give rise to a compensating motion of the electrons in the field. At ultrasonic frequencies so far employed in practice it has been shown[14,19] that a quasibalance condition is imposed on the net ionic and electronic current $\mathbf{j}$. It is, however, important to note a distinction between the longitudinal and transverse interactions. In the former case the electric field arises as a consequence of the density modulation of the lattice points; the charge imbalance, arising from the incomplete following (by electrons) of the time-varying displacement of ionic cores, is associated directly with the local electric fields. In the transverse-wave case there is assumed no density modulation for small particle displacements, the polarization now being transverse to the propagation vector, and the local electric field is generated by induction. But due to the Meissner effect the electric field is effectively extinguished in the superconducting state, at all temperatures except in the immediate vicinity of T_c. Since the ultrasonic wavelengths λ generally lie in the range 10^{-2}–10^{-3} cm, it is clear that as soon as the range of $\mathbf{B}$ is reduced well below the order of 10^{-3} cm the electromagnetic interaction will be effectively shut off. One way of evaluating the stringency of this condition qualitatively is to examine it in light of the temperature dependence of the penetration depth δ in a superconductor. This may be expressed roughly, in terms of the London theory,[23] as

$$\delta(t)=\delta(0)(1-t^4)^{-1/2},$$

where, typically, $\delta(0)\sim 10^{-6}$ cm. Cooling from $t=1$ to $t=0.999$ corresponds to a reduction of δ from ∞ at T_c to approximately 10^{-5} cm. Thus, at a temperature 0.001 t below T_c the condition $\delta\ll\lambda$ has already been attained, and electromagnetic interaction has become negligible.

Consider the manner in which the "real" electromagnetic force enters in the Pippard theory for the normal-state attenuation of acoustic waves by an arbi-

[23] F. London, *Superfluids* (John Wiley & Sons, Inc., New York, 1954), Vol. I.

trary Fermi surface. The net fictitious force π' gives rise to an electronic current J, when viewed from the frame fixed in the lattice. To satisfy the current quasibalance condition a self-consistent electric field $\mathbf{E}$ is generated such that the sum of real and fictitious forces ($e\mathbf{E}$ and π', respectively) results in zero net current. Given a force π, real or fictitious, the corresponding current is,[19] in absence of a magnetic field,

$$\mathbf{J}=\frac{e}{4\pi^3\hbar}\int\frac{\pi\mathbf{l}dS}{1-ia\cos\varphi}, \tag{12}$$

where $i\omega\tau$ has been neglected in the denominator since it is generally much less than 1; $\omega\tau=a(V_s/V)$, and $V_s/V\sim10^{-2}$ to 10^{-3} in a metal.

Since it is the current $\mathbf{J}$ given by substituting π' in Eq. (12) which must be neutralized, the electric field required to establish current balance is

$$E_j=-\frac{ie}{4\pi^3}\rho_{ij}\int a_i\left(\frac{\mathbf{D}\cdot\mathbf{u}}{1-ia\cos\varphi}\right)dS, \tag{13}$$

where $a_i=ql_i$. Since E_p, the electric field component parallel to the electronic motion, is $\mathbf{E}\cdot\mathbf{a}/a$ and the current vector represented in the last equation is J_i, Eq. (13) may be rewritten

$$E_p=E_j\frac{a_j}{a}=\frac{e}{4\pi^3a}\rho_{ij}a_j\int a_i\left(\frac{\mathbf{D}\cdot\mathbf{u}a\cos\varphi}{1+a^2\cos^2\varphi}\right)dS. \tag{13'}$$

Since the corresponding force is eE_p, the total force π on an electron parallel to its motion, viz., normal to the Fermi surface, is

$$\pi=\pi'+eE_p.$$

Thus

$$\pi=iq\hbar\mathbf{D}\cdot\mathbf{u}+\frac{e^2}{4\pi^3a}\rho_{ij}a_j\int a_i\left(\frac{\mathbf{D}\cdot\mathbf{u}a\cos\varphi}{1+a^2\cos^2\varphi}\right)dS. \tag{14}$$

From this net force, the corresponding displacement of the Fermi surface may be calculated. The attenuation associated with relaxation of the displaced Fermi surface has already been given in Eq. (9).

The second term of Eq. (14) is to be associated with the second term of Eq. (9); they arise from the introduction of a real electric field, the magnitude of which is determined on the assumption of a current quasibalance condition. It has been noted, however, that when this electric field is associated with transverse phonons, it cannot be supported in a superconductor at temperatures below the immediate region of T_c: the Meissner effect results in a strong screening of the transverse electric fields. Thus, over almost the entire superconducting region real electric fields are screened, and the current associated with the fictitious force π' is not compensated. The force, given by Eq. (14) reduces to

$$\pi=iq\hbar\mathbf{D}\cdot\mathbf{u},$$

and the corresponding expression for the attenuation [recall Eq. (9)] becomes

$$\alpha=\frac{\hbar q}{4\pi^3Mv_s}\int\frac{\mathfrak{D}^2qldS}{1+(ql)^2\cos^2\varphi}.$$

At temperature T_R, then, which may now be defined as that temperature (below T_c) below which the electromagnetic interaction is negligible, the corresponding attenuation is α_R. Recalling that $T_R/T_c\approx0.999$, we may write

$$\alpha_R(T_c)\approx\frac{\hbar q}{4\pi^3Mv_s}\int\frac{\mathfrak{D}^2qldS}{1+(ql)^2\cos^2\varphi}. \tag{15}$$

What has been done, then, is to turn off electromagnetic interaction in order to describe the electron-shear-wave interaction in the superconducting state at T_c. When the attenuation term corresponding to the electromagnetic force in the Pippard treatment is identified and removed, there remains the contribution corresponding to the so-called *residual* superconducting attenuation α_R, which contains both the collision-drag and shear-deformation interactions. (Recall Ref. 22.)

The collision-drag contribution. In the free-electron treatment of Claiborne and Morse[13] it was found that, for transverse waves in an ideal free-electron metal, the total residual attenuation α_R is given by Eq. (2). It is of interest to attempt to apply the present considerations, which treat the more general case of an arbitrary Fermi surface, to that problem. We have asserted that the electromagnetic interaction is effectively shut off by Meissner effect below T_R with the result that the residual attenuation must be expressed by Eq. (15). Thus, at T_c, we assert that the relative residual attenuation for transverse phonons is approximately

$$\frac{\alpha_R}{\alpha_{nt}}=\int\frac{\mathfrak{D}^2adS}{1+a^2\cos^2\varphi}\Bigg/\int\left[\frac{\mathfrak{D}^2adS}{1+a^2\cos^2\varphi}+\frac{e^2}{4\pi^3hq}\rho_{ij}{}^q\right.$$
$$\left.\times\int ql_i\left(\frac{\mathfrak{D}a\cos\varphi}{1+a^2\cos^2\varphi}\right)dS\int\left(\frac{\mathfrak{D}a\cos\varphi}{1+a^2\cos^2\varphi}\right)ql_jdS\right]. \tag{16}$$

Recalling that $\mathfrak{D}=\mathbf{D}\cdot\mathbf{u}/u$, the deformation parameter $\mathfrak{D}$ for the case of pure shear is given by

$$\mathfrak{D}=K_{xy}+k_y\cos\varphi$$

if the particle velocity is taken to be along the y axis. In the ideal free-electron metal $K_{xy}=0$ and $\mathfrak{D}=k_y\cos\varphi$. The angles introduced in writing the surface element dS are defined in Fig. 2. Note that, as before, x is the propagation direction and y is the polarization direction for pure shear. To evaluate the integral for the free-electron case, the following identifications may therefore be made: (1) $K_{xy}=0$, (2) $k_y=k\sin\varphi\cos\psi$, with k a constant, and (3) $\mathfrak{D}=k_y\cos\varphi$. The attenuation ratio be-

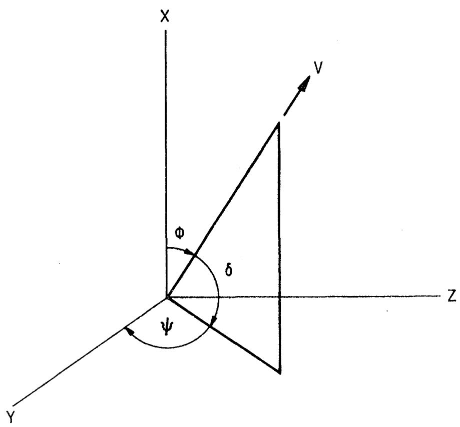

FIG. 2. Orientation of Fermi velocity **V** relative relative to coordinate axes.

comes, in the free-electron limit,

$$\left(\frac{\alpha_R}{\alpha_{nt}}\right)'=\left[1+\left(\frac{a}{k}\right)^2\frac{P}{Q}\right]^{-1}, \tag{17}$$

where

$$P=ak^4\int_0^\pi \frac{\sin^3\varphi\cos^2\varphi d\varphi}{1+a^2\cos^2\varphi}\int_0^{2\pi}\cos^2\psi d\psi$$

and

$$Q=ak^2\int_0^\pi \frac{\sin^3\varphi d\varphi}{1+a^2\cos^2\varphi}\int_0^{2\pi}\cos^2\psi d\psi;$$

the prime is used to signify that α_R/α_{nt} in Eq. (17) refers to the free-electron case. Thus

$$\left(\frac{\alpha_R}{\alpha_{nt}}\right)'=\left[1+a^2\left(\int_0^\pi \frac{\sin^3\varphi\cos^2\varphi d\varphi}{1+a^2\cos^2\varphi}\right)\Big/\left(\int_0^\pi\frac{\sin^3\varphi d\varphi}{1+a^2\cos^2\varphi}\right)\right]. \tag{18}$$

Equation (18) reduces (see Appendix I) to

$$(\alpha_R/\alpha_{nt})'=g, \tag{19}$$

where the parameter g is defined in Eq. (3). In the same free-electron limit, of course, from Eqs. (11) and (19),

$$\alpha_E/\alpha_n=1-g. \tag{20}$$

Thus we find, by turning off the electromagnetic interaction and taking the problem to the free-electron limit, that the result, Eq. (19), is identical to that derived in the ideal free-electron case by Clairborne and Morse[13] for the residual superconducting shear-wave attenuation, attributable to collision drag. It is to be noted that, from the point of view of the frame fixed in the lattice, it is the fictitious force π^1, corresponding to the "relative-velocity effect," which is responsible for the presence of a residual attenuation in the ideal, free-electron case.

The shear-deformation interaction. We return now to the general case of the arbitrary Fermi surface. The deformation parameter K_{xy} is no longer zero, and the deformation contribution to Eq. (15) which we shall define as $\alpha_D(T_c)$ is

$$\alpha_D(T_c)=\frac{\hbar q}{4\pi^3Mv_s}\oint\frac{aK_{xy}(K_{xy}+2k_y\cos\varphi)dS}{1+a^2\cos^2\varphi}. \tag{21}$$

As a becomes large the integral contributes significantly to α_D only for portions of the Fermi surface which correspond to "effective zones," viz., only where $\varphi\approx\frac{1}{2}\pi$. It is seen from Fig. 2 that on the effective zones the Fermi surface is tangent to the phonon propagation vector $\mathbf{q}$. Since the Fermi velocity $\mathbf{v}$ in a typical metal is much greater than that of the acoustic wave ($V/V_s\sim10^2$ to 10^3), the effective zones represent the portions of the Fermi surface where electrons can interact strongly since they move essentially in phase with the acoustic wave for relatively long times. Since $\delta=\frac{1}{2}\pi-\varphi$ (see Fig. 2), $\alpha_D(T_c)$ becomes, for $a\gg1$,

$$\alpha_D(T_c)\approx-\frac{\hbar q}{4\pi^3Mv_s}\int\int\frac{RK_{xy}{}^2ad\delta d\psi}{1+a^2\delta^2};$$

R is the product of the principal radii of curvature and $K_{xy}(\psi)$ is evaluated on the effective zone, where $\varphi\approx\frac{1}{2}\pi$ or $\delta\approx0$. The integration over δ yields the factor $-\pi$. Thus, for $a\gg1$,

$$\alpha_D(T_c)\approx\frac{\hbar q}{4\pi^2Mv_s}\oint RK_{xy}{}^2d\psi. \tag{22}$$

Hence, in the range $ql\gg1$ the deformation part α_D of the residual attenuation α_R is determined by electron-phonon interaction confined to the effective zones.

In contrast, the collision-drag part of the attenuation, obtained from Eq. (15) by letting $K_{xy}=0$, is

$$\alpha_c\approx\alpha_R(T_c)'=\frac{\hbar q}{4\pi^3Mv_s}\int\frac{ak_y{}^2\cos^2\varphi dS}{1+a^2\cos^2\varphi}. \tag{23}$$

And it is clear that for $a\gg1$, in contrast to the case for α_D, almost the entire Fermi surface contributes. Thus, for $a\gg1$,

$$\alpha_c\approx\frac{\hbar}{4\pi^3Mv_s}\int\frac{k_y{}^2}{l}dS. \tag{24}$$

In fact since the element dS contains $\sin\varphi$ as a factor, there is no contribution to α_c on the effective zone itself. Thus, the residual attenuation of transverse acoustic waves by excited quasiparticles is separable into a collision-drag and a shear-deformation contribution; for $a\gg1$, the region of the Fermi surface which contributes to α_D is confined to the effective zones, while the remainder of the surface determines α_c.

"Frequency separation" of shear deformation and collision drag. It is clear from the foregoing discussion that α_D and α_c may be separated experimentally by means of measurements on the frequency dependence of phonon absorption in the superconducting state. The normal-state transverse-wave absorption α_{nt} is proportional to phonon frequency when $a \gg 1$, even for the case of an arbitrary Fermi surface, since Eq. (9) reduces (for pure shear waves) in that limit to[19]

$$\alpha_{nt} \approx \frac{\hbar q}{4\pi^2 M v_s} \left\{ \oint R K_{xy}{}^2 d\psi + \frac{1}{\pi^2} \frac{\left[\int \mathfrak{D} \tan\varphi \cos\psi dS \right]^2}{\oint R \cos^2\psi d\psi} \right\}. \quad (25)$$

It is seen from Eqs. (24) and (25), that $\alpha_c(T_c)/\alpha_{nt}$ is a monotone-decreasing function of frequency of the acoustic wave, while [see Eq. (22)] $\alpha_D(T_c)/\alpha_{nt}$ is independent of ql. Since $\alpha_D + \alpha_c = \alpha_R$, measurements of α_R/α_{nt} versus ql in the superconducting state can extract the ql-independent deformation contributions, represented by Eq. (22). Thus, from measurements of the residual attenuation in the superconducting state, the absorption can be related to the deformation parameter on effective zones. By taking advantage of the cancellation of the electromagnetic interaction in the superconducting state it is thus possible to extract conditions for which measurements of electronic attenuation of transverse acoustic waves are connected in a relatively direct way to the shear deformation properties of the Fermi surface. In the case of the normal-state attenuation only the longitudinal attenuation coefficient α_{nl} can be reduced to such a form; α_{nt} [see Eq. (25)] is determined by contributions from the whole Fermi surface, even in the limit $a \gg 1$.

It is important to recognize the following property[19] of shear-deformation contributions on effective zones: There are no contributions to Eq. (22) from effective zones which lie on planes of reflection symmetry for the Fermi surface since $\mathfrak{D} = 0$ in such regions. Thus, for example, $\alpha_D = 0$ in the case of the spherical Fermi surface of an ideal free-electron metal. In real cases, however, Fermi surfaces are more complex and there is reasonable probability of finding effective zones which do not satisfy reflection symmetry. Shear deformation is thus expected in general to contribute to the total electron-phonon interaction. This is expected to be especially true in superconductors, which are usually polyvalent and have Fermi surfaces that are large relative to the Brillouin zone. In the superconducting state the shear deformation contribution over effective zones becomes the only source of electronic attenuation when a is large.

IV. APPLICATION TO EXPERIMENTAL RESULTS

Experimental studies of electronic attenuation of acoustic waves by electrons (especially for the $\mathbf{H} = 0$ case) have generally been evaluated from the point of view of the ideal free-electron case, for which $K_{xy} = 0$ everywhere on the Fermi surface and only components of the form $K_{ij}\delta_{ij}$ are associated with absorption. It has been noted, however, that, for effective zones not associated with planes of mirror symmetry of the Fermi surface, shear deformation does contribute. Thus it is of interest to examine the experimental evidence for shear-deformation contributions; and to consider the possibilities for investigating shear-deformation effects from measurements in the superconducting state, using the methods developed in the foregoing analysis.

Tin. In a preliminary investigation of shear-deformation effects by the present author in superconducting tin[1] it became quite clear that relatively large values of α_D contribute to the shear-wave attenuation. The measured values of α_R/α_{nt} were not describable in terms of the ideal free-electron prediction represented by Eq. (2), and it was proposed that a ql-independent term, large for the case of tin, was also required. It was concluded that in superconducting tin electron-phonon interaction associated with shear deformation of the Fermi surface contributes significantly to the observed ultrasonic attenuation, and that the effect of collision drag on the residual shear-wave superconducting attenuation is inadequate alone to account for the observations in tin.

Large values of α_D/α_{nt} are to be expected in tin. The free-electron sphere in k space completely encloses the first Brillouin zone, and intersects Brillouin zone faces to the sixth zone.[24] Deformation contributions to the absorption of the acoustic wave are favored near regions of intersection with the Brillouin zone boundaries due to the low Fermi velocities which occur there. At the same time the condition $\delta = 0$, defining the effective zones, is often satisfied only on a central section and certain of the regions of intersection with the Brillouin zone boundaries. A specific illustration is treated below for the case of aluminum. Although effective zones satisfying mirror symmetry do not contribute to the shear-wave attenuation, it may be assumed for a Fermi surface such as that of tin that, for a given propagation direction, there are likely also to be found effective zones which do not obey the symmetry condition. The Fermi surface of tin is so complex and poorly understood at present that it is perhaps not fruitful to attempt even a qualitative identification of shear deformation contributions with portions of the Fermi surface. This may not be the case for aluminum, however.

Aluminum. David *et al.*[2] repeated the shear-wave superconducting attenuation experiments of Claiborne discussed in Chap. I, comparing their data against Eq. (2). Since $(T_c - T_R)/T_c \sim 0.001t$, the approximation[22] $2F[\Delta(T_R)] = 1$, implicit in Eq. (2′), is valid to within

[24] A. V. Gold and M. G. Priestley, Phil. Mag. **5**, 1089 (1960).

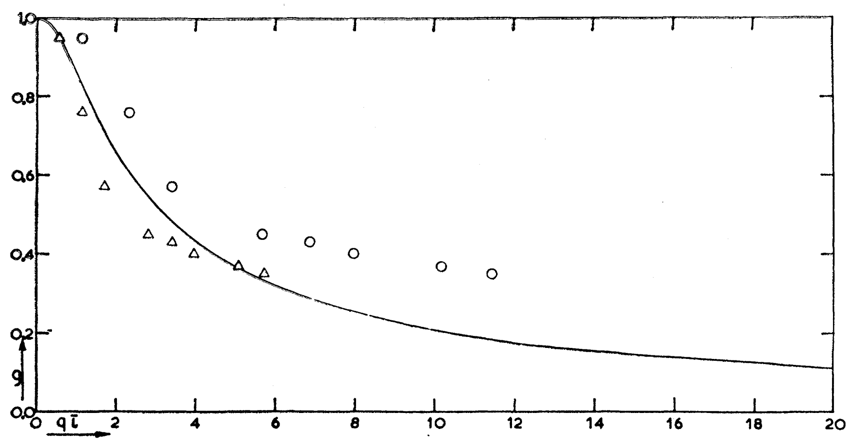

FIG. 3. ql dependence of the function g and α_R/α_{nt} data on aluminum [after David *et al.*, (Ref. 2) slightly modified].

approximately 1%. In Fig. 3, after David *et al.*,[2] both g and the experimentally determined α_R/α_{nt} values are plotted against ql. The data given by the "circles" are represented in terms of ql rather than frequency by assuming an effective electron mean free path, l, of 0.024 cm; it was determined that $ql=1$ at a frequency of 2.2 Mc/sec, the ultrasonic velocity being 3.3×10^5 cm/sec. It is clear that Eq. (2) is not satisfied. The data represented by "triangles" also were included to demonstrate that halving the mean free path leads to even poorer agreement. David *et al.* concluded that agreement with the theory as represented by Eqs. (2) and (2′) is poor.

The disagreement between experiment and theory represented in Fig. 3 can be readily understood in terms of the analysis presented in Sec. IIIB. In Eqs. (22), (24), and (25) it was seen that in the limit $ql\gg1$ only the collision-drag contribution α_c/α_{nt} reduces to zero, while α_D/α_{nt} becomes a constant independent of ql. It is to be noted in Fig. 3 that the divergence of the data points from the $g(ql)$ curve becomes greater at large ql values.

The expression for α_R/α_{nt} applicable to real Fermi surfaces and arbitrary ql depends on $\mathfrak{D}$ in a rather complicated way [see Eq. (16)]. In order to apply the results of the more general model to the aluminum data of David *et al.* (see Fig. 3) over the range of ql values, it is therefore necessary to make a simplifying assumption. Claiborne and Morse, in treating their aluminum data, assumed an ideal free-electron model, obtained Eq. (2), and found reasonable agreement with experiment. The data of David *et al.* perhaps because the ql range covered is somewhat greater, find deviations. From theory and experiment[25–27] the aluminum Fermi surface is expected not to deviate greatly from an ideal free-electron sphere. Hence, guided by the results of the general model given in Sec. (IIIB), we take as the next level of approximation

$$\alpha_R/\alpha_{nt}\approx cg+d. \tag{26}$$

The parameter d represents an essentially ql-independent deformation term, and cg is the collision-drag term; c is a weighting coefficient which guarantees the condition

$$c+d=1. \tag{27}$$

Thus, the limiting requirements imposed by the general model are satisfied: α_R/α_{nt} goes to 1 as ql goes to zero; in the limit of large ql, α_R/α_{nt} reduces to a ql-independent deformation term; and the ql dependence of collision drag is represented by g—which, as was shown in the discussion preceding Eq. (17), is strictly correct only in the free-electron limit.

In Fig. 4 (after David *et al.*[2]) the α_{nt} data corresponding to the circled points in Fig. 3 are shown as a function of frequency. The solid curve represents the frequency dependence of normal-state attenuation in the theory of Pippard [see Eq. (4)]. As a test of Eq. (26), α_R/α_{nt} is plotted versus $g(ql)$ in Fig. 5. The error bars are based on the estimate of David *et al.* that an error of about 5% was incurred in independent determinations of attenuation. (The solid circles were obtained after smoothing of the *normal-state* attenuation to the Pippard theory in Fig. 4.) It is seen that the function represented in Fig. 5 is of linear form, as required, and there is obtained a positive intercept on the ordinate, which would appear to give evidence for a shear-deformation term. However, the data would suggest that as ql goes to zero α_R/α_{nt} becomes greater than 1, which is of course impossible by definition. Note, however, that primary data were determined in terms of frequency and not ql; the ql scale was inferred by David *et al.* essentially by a slide fit technique, from which it was determined that $ql=1$ at 2.2 Mc/sec. This corresponded to a derived electron mean free path l of 0.024 cm. Clearly, an error in this procedure can result in ql-scale error, which corresponds to error in the determination of electron mean free path. We examine the case $ql'=0.70\ ql$. The scale change, represented by the factor 0.70, corresponds to the assumption of a new mean free path l', where $l'=0.017$ cm. An effective electron mean free path of 0.017 cm is no less reasonable

[25] See, for example. W. A. Harrison, Phys. Rev. **118**, 1182 (1960).
[26] B. W. Roberts, Phys. Rev. **119**, 1889 (1960).
[27] G. N. Kamm and H. V. Bohm, Phys. Rev. **131**, 111 (1963).

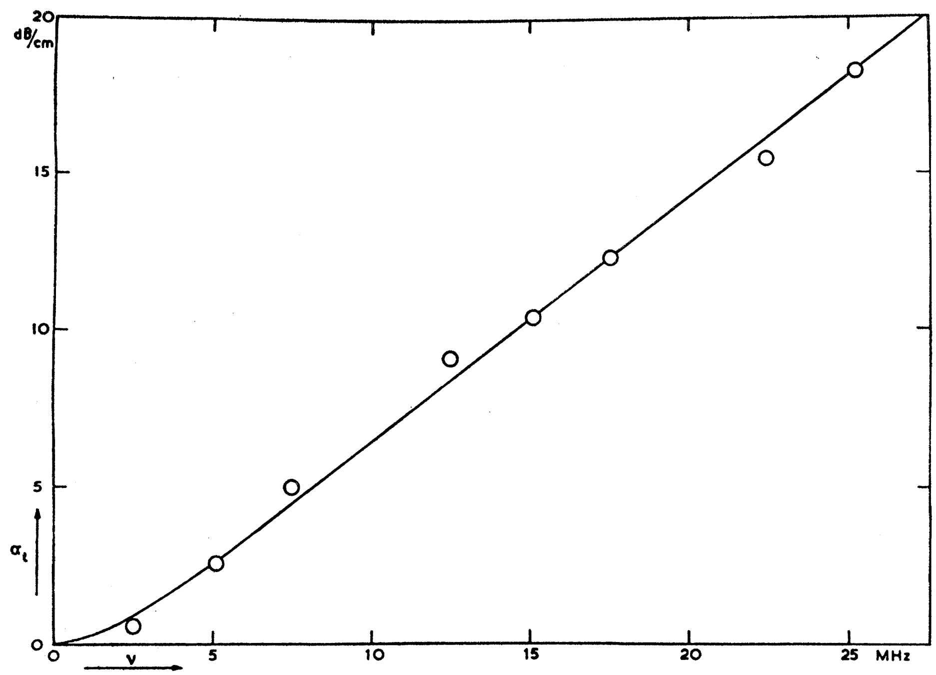

FIG. 4. Normal-state shear-wave attenuation versus frequency [after David *et al.* (Ref. 2)].

than one of 0.024 cm since the acoustic experiments are incapable of choosing between them; and the scale shift corresponding to the factor 0.70 is not inconsistent with the indicated error associated with determinations of attenuation.

In Fig. 6 α_R/α_{nt} is plotted versus $g(ql')$. The data are still satisfied by a straight line, but now, in addition, the required normalization condition is met, viz., $\alpha_R/\alpha_{nt}=1$ when $ql=0$. In accordance with Eq. (26) the curve satisfies a linear form and has a positive intercept on the ordinate. Equation (26) is seen to describe the data represented in Fig. 3 reasonably well. The reasonable success of the approximations embodied in Eq. (26) may be attributed to the fact that the aluminum Fermi surface does not deviate greatly from a free-electron sphere. Thus, the shear deformation term is small and the collision drag effect is approximated by a function of the form $g(ql)$.

A shear-deformation contribution of about 10% is suggested since $d\sim 0.01$. However, the uncertainties regarding the ql scale in Figs. 5 and 6 make it clear that the inferred value of the deformation term cannot be regarded as very accurate. In any case, to determine the magnitude of the deformation term it is far better to follow another procedure, which is applicable to real Fermi surfaces and does not rest on the approximations inherent in Eq. (26): As seen from Eqs. (22) and (25),

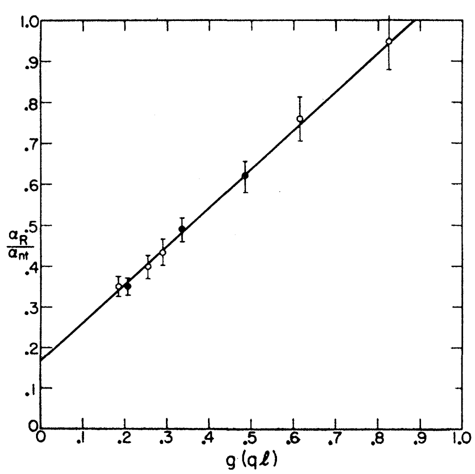

FIG. 5. α_R/α_{nt} versus $g(ql)$. The experimental points are computed from data reported by David *et al.* on aluminum.

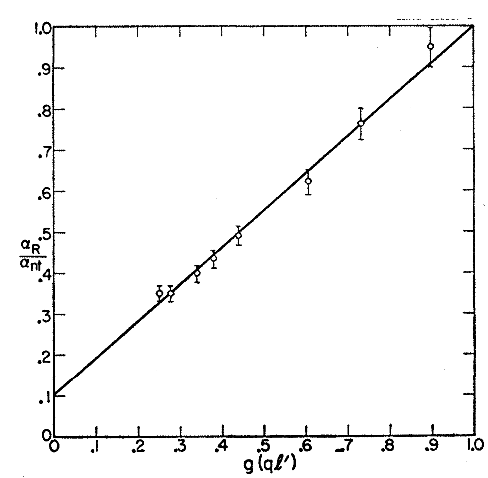

FIG. 6. α_R/α_{nt} versus $g(ql')$. The experimental points refer to data of David *et al.* on aluminum. A modified mean free path l' is used in this representation.

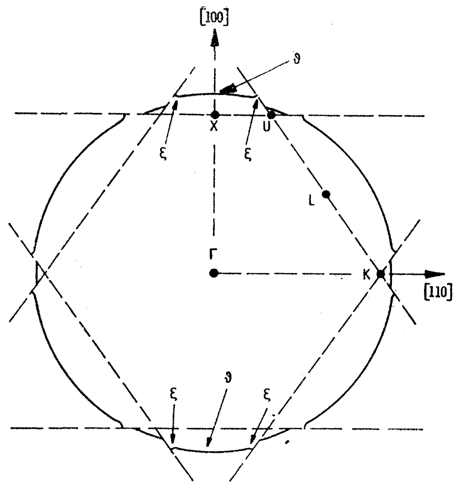

FIG. 7. The Fermi surface for aluminum in the extended-zone scheme. Shown is the intersection of the Fermi surface with a central (110) plane. The dashed lines represent Bragg-reflection planes (after Harrison).

the deformation contribution is given by the ratio α_R/α_{nt} in the limit $a\gg 1$.

Transition metals. The absence of a region I (see Fig. 1) in experiments on transition metals can be understood in terms of the proposed model. In the case of the shear-wave measurements of superconducting attenuation in transition metals by Levy, Kagiwada, and Rudnick[16] and by Dobbs (private communication) $ql<1$ in all cases. For $ql<1$, $g\approx 1$ and it is seen from the free-electron prediction [Eq. (2)] that $\alpha_R\approx\alpha_{nt}$. In terms of an equivalent argument Levy attributed the absence of region I in his transition metal data to the condition $ql<1$. The present model, which is applicable to real Fermi surfaces, also satisfies these observations. In the theory of Pippard for the normal-state attenuation, it is shown that the second term of Eq. (9) becomes negligible for $a\ll 1$. In the case $a\ll 1$, therefore, we may write

$$\alpha_{nt}=\frac{\hbar q^2}{4\pi^3 M v_s}\int \mathfrak{D}^2 l dS\,, \tag{28}$$

and, recalling Eq. (16), it is seen that $\alpha_R/\alpha_{nt}\approx 1$. We find, then, that in the present treatment both the ideal free-electron reduction of α_R/α_{nt}, viz., Eq. (19), and the general case of real Fermi surfaces predict α_R/α_{nt} when $ql\ll 1$.

Gallium. The apparently anomalous results in gallium obtained by Hart and Roberts[17] cannot be understood in terms of the free-electron model. Even the present generalization is probably inadequate to treat the experimental results for the case of gallium in detail. As has been pointed out, it was found for most orientations of the acoustic wave relative to the lattice that $\alpha_R\approx\alpha_{nt}$, i.e., the rapid-fall and residual attenuation regions were of comparable magnitude; and there was found no frequency dependence of the relative magnitudes of regions I and II despite the fact that the frequencies ranged from 10 to approximately 300 Mc/sec. Yet, for all frequencies and orientations, $ql>100$.

Now the free-electron prediction, Eq. (2), would suggest $\alpha_R/\alpha_{nt}\approx 0$ for such large ql values. In the present model, however, in the range of large ql values it is seen from Eqs. (22), (24), and (25) that α_c/α_{nt} goes to zero, while α_D/α_{nt} becomes independent of ql and is given by

$$\frac{\alpha_D}{\alpha_{nt}}=\oint RK_{xy}^2 d\psi\bigg/\bigg[\oint RK_{xy}^2 d\psi+\frac{1}{\pi^2}\times\bigg(\int \mathfrak{D}\tan\varphi\cos\psi dS\bigg)^2\bigg/\oint R\cos^2\psi d\psi\bigg]. \tag{29}$$

This constant term thus accounts for the presence of a residual attenuation even at very large ql values. As in the case of tin, the shear deformation contribution is quite large, α_D/α_{nt} being typically 0.4 or greater for most propagation orientations. As in tin, the Fermi surface of gallium is very complex, the proliferation of nearly-free-electron reduced-zone sections being even greater than for the former metal. There remains to be explained the absence of a rapid-fall region for one specific acoustic wave orientation, and the appearance of anomalies in the "shape" of the rapid-fall region.[17]

Sources of shear deformation. It was noted earlier that effective zones which lie on planes of reflection symmetry of the Fermi surface cannot contribute[19] to the shear-deformation attenuation, and that those which do not have such symmetry may often be found near regions of intersection with Brillouin zone boundaries. It is perhaps useful to illustrate these conditions for the aluminum data treated earlier. The data represented in Fig. 3 correspond to propagation of the acoustic wave along [110] and polarization along the [100] crystalline axis. The relevant section of the unfolded Fermi surface, shown in Fig. 7, is that cut by a central (110) plane. The propagation vector **q** can be viewed as either directed into the paper at point Γ or along Γ*K*; sections corresponding to rotation by 90° about Γ*X* are equivalent. Let us for the moment regard **q** as being along Γ*K*, so that the effective zones are viewed in cross section. The effective zones may be readily identified as the closed paths on the surface which are essentially tangent to **q**. The zone labeled θ (on the central section) gives no shear-deformation contribution due to reflection symmetry. However this is not the case for the noncentral effective zones, and their contribution can be large since they lie near intersections with Brillouin zone boundaries. The points ξ identify a portion of such an effective zone, which portion can be seen, by means of a rotation by 90° about Γ*X*, to correspond to the segments ξ–ξ at the top and bottom of the figure. The remainder of the closed path, not easily visualized from Fig. 7, can be traced with the aid of the corresponding three-dimensional reduced-zone surface.

This example serves to illustrate the nature of the selectivity available in the superconducting shear-deformation interaction. It has been shown that in the superconducting state, when $ql \gg 1$, the shear-wave attenuation by electrons can be attributed entirely to shear-deformation interaction *confined to effective zones*, and that the measured attenuation bears a simple relation to the shear-deformation parameter [see Eq. (22)]. At the same time, it is to be recalled that, unlike the interaction involving longitudinal phonons, not all effective zones contribute to the deformation interaction of electrons with transverse phonons; a symmetry condition excludes zones coinciding with planes of mirror symmetry of the Fermi surface. It is, therefore, concluded that it is possible in principle to identify shear-wave attenuation measured in the superconducting state with a select and identifiable (in the case of simple Fermi surface) group of electrons. We are preparing in indium to make shear-wave measurements suggested by some of the foregoing considerations.

The temperature dependence of the shear-wave residual attenuation. The BCS prediction give by Eq. (1) applies to longitudinal acoustic-wave absorption for the case $ql \gg 1$, and is found to follow when the normal-state electron-phonon scattering is of the form

$$\alpha_{nl} \sim \oint R D_{xx}{}^2 d\psi \,,$$

where the integral is taken about effective zones. It has been noted by Pippard[19] that the transverse-wave absorption α_{nt} does not reduce to such a simple form, even in the case $ql \gg 1$ [see Eq. (25)], and that as a consequence transfer of the BCS argument to this transverse wave interaction must be applied with caution.

However, in experiments on a number of superconductors[1,2,4,12,16] it has been found that the residual shear-wave attenuation ratio $\alpha_r(T_i)/\alpha_{nt}$ (recall Fig. 1) satisfies Eq. (1) rather well; the BCS relation has been found to be quite as successful in fitting (residual) shear-wave data as that for longitudinal waves. This may perhaps be understood in light of the discussion in Sec. III.B concerning electromagnetic interaction. It was seen that the electromagnetic interaction is effectively shut off below temperature T_R (see Fig. 1), thus causing the second term in Eq. (25) to disappear. It has also been noted that for $ql \gg 1$ the collision-drag effect, which involves virtually the entire Fermi surface, does not contribute, so that the presence of a residual attenuation must be attributed entirely to shear-deformation interaction.

When $ql \gg 1$, the effective form of α_{nt} immediately below T_c, then, is simply [recall Eq. (22)]

$$\alpha_{nt} \approx \alpha_D(T_c) = \frac{\hbar q}{4\pi^2 M v_s} \oint R K_{xy}{}^2 d\psi \,,$$

which is a form identical to that corresponding to α_{nl}. Thus, it is possible to account for the applicability of Eq. (1) both to α_{sl}/α_{nl} and α_r/α_{nt}, for the case $ql \gg 1$. In other words, the form of the shear-deformation contribution to the residual attenuation indicates the applicability of the BCS relation to the case of the superconducting transverse wave residual attenuation when $ql \gg 1$.

CONCLUSIONS

Collision drag and shear deformation must be described simultaneously in order to account for the general features of observed electronic attenuation of transverse acoustic waves in the superconducting state. An analysis which takes explicit account of the shear-deformation effect has been performed in order to provide a quantitative application of this idea to experimental data. A model which introduces both interactions explicitly and provides a description of the residual shear-wave attenuation at T_c is obtained by turning off electromagnetic interaction within the Pippard formalism describing the normal state. In application of the analysis to given data on aluminum, the shear-deformation effect is found to account for roughly 10% of the total electronic interaction at low temperatures.

It is found for "real" Fermi surfaces, viz., Fermi surfaces for which there is a shear-deformation contribution, that the residual attenuation ratio, α_R/α_n, has the following properties:

(1) The ratio goes to 1 for $ql \ll 1$.

(2) As ql increases, the collision-drag contribution diminishes and the ratio α_R/α_n reduces in magnitude; in the limit $ql \gg 1$, the ratio approaches a constant value α_D/α_n, the shear-deformation contribution.

(3) If the free-electron limit is taken, it is found that the ratio α_R/α_n reduces to g, in agreement with the free-electron result of Morse and Claiborne. At the next level of approximation suggested by the present model, the aluminum data of David, van der Laan, and Poulis are found to be reasonably well satisfied.

The deformation contribution is seen to take a relatively simple form [recall Eq. (22)] in the superconducting state when $ql \gg 1$. It is thus suggested that the shear-deformation properties of the Fermi surface may be studied experimentally by measuring electronic attenuation of transverse acoustic waves in the superconducting state. In the normal-state electromagnetic interaction must also be considered, and the connection between attenuation data and the shear-deformation parameter is much more indirect [recall Eq. (25)]. It is also to be noted that the form of Eq. (22) makes it possible to understand—at least for the case $ql \gg 1$—the sucsuccess of the BCS relation, Eq. (1), in satisfying shear-wave data in the residual attenuation region.

Some of the foregoing considerations have motivated an experimental study in which we hope to investigate shear-deformation properties of Fermi surfaces.

ACKNOWLEDGMENTS

The author is indebted to T. D. Holstein for a number of illuminating discussions. He also wishes to thank M. Ashkin, M. Pollak, and J. A. Rayne for helpful conversations.

APPENDIX I

The integrals may be reduced to simple standard forms by means of the substitution $u=\cos\varphi$. Thus the first integral in Eq. (18) becomes

$$\frac{1}{a^2}\int_1^{-1} u^2du-\frac{1}{a^2}\left(1+\frac{1}{a^2}\right)\times\int_1^{-1} du+\frac{1}{a^2}\left(\frac{1}{a^2}+1\right)\int_1^{-1}\frac{du}{1+a^2u^2},$$

and the second integral in Eq. (18) reduces to

$$\frac{1}{a^2}\int_1^{-1} du-\left(1+\frac{1}{a^2}\right)\int_1^{-1}\frac{du}{1+a^2a^2}.$$

Since

$$\int_1^{-1}\frac{du}{1+a^2u^2}=-\frac{2}{a}\arctan a,$$

$$\left(\frac{\alpha_R}{\alpha_{nt}}\right)'=\left\{1+a^2\left\{\left[\frac{2}{a^2}\left(1+\frac{1}{a^2}\right)\left(1-\frac{1}{a}\arctan a\right)-\frac{2}{3a^2}\right]\Big/\left[2\left(1+\frac{1}{a^2}\right)\left(\frac{1}{a}\arctan a\right)-\frac{2}{a^2}\right]\right\}\right\}^{-1}.$$

In terms of the parameter g, where [recalling Eq. (3)] g is given by

$$g=(3/2/a^2[((a^2+1)/a)\arctan a-1],$$

the residual attenuation ratio is

$$(\alpha_R/\alpha_{nt})'=[1+(1-g)/g]^{-1},$$

or

$$(\alpha_R/\alpha_{nt})'=g, \qquad (19)$$

in agreement with Eq. (2).